

Ultralow nanoscale wear through atom-by-atom attrition in silicon-containing diamond-like carbon

Harish Bhaskaran^{1*}†, Bernd Gotsmann¹, Abu Sebastian¹, Ute Drechsler¹, Mark A. Lantz¹, Michel Despont^{1*}, Papot Jaroenapibal^{2†}, Robert W. Carpick², Yun Chen^{3†} and Kumar Sridharan³

Understanding friction^{1–4} and wear^{5–11} at the nanoscale is important for many applications that involve nanoscale components sliding on a surface, such as nanolithography, nanometrology and nanomanufacturing. Defects, cracks and other phenomena that influence material strength and wear at macroscopic scales are less important at the nanoscale, which is why nanowires can, for example, show higher strengths than bulk samples¹². The contact area between the materials must also be described differently at the nanoscale¹³. Diamond-like carbon is routinely used as a surface coating in applications that require low friction and wear because it is resistant to wear at the macroscale^{14–20}, but there has been considerable debate about the wear mechanisms of diamond-like carbon at the nanoscale because it is difficult to fabricate diamond-like carbon structures with nanoscale fidelity. Here, we demonstrate the batch fabrication of ultrasharp diamond-like carbon tips that contain significant amounts of silicon on silicon microcantilevers for use in atomic force microscopy. This material is known to possess low friction in humid conditions, and we find that, at the nanoscale, it is three orders of magnitude more wear-resistant than silicon under ambient conditions. A wear rate of one atom per micrometre of sliding on SiO₂ is demonstrated. We find that the classical wear law of Archard²¹ does not hold at the nanoscale; instead, atom-by-atom attrition^{7,8} dominates the wear mechanisms at these length scales. We estimate that the effective energy barrier for the removal of a single atom is ~ 1 eV, with an effective activation volume of $\sim 1 \times 10^{-28}$ m³.

Rather than coating nanoscale tips with wear-resistant materials, we used a moulding technique^{22–24} to fabricate monolithic ultrasharp tips of diamond-like carbon with silicon (Si-DLC) on standard silicon microcantilevers. This is a bulk processing technique that has the potential to scale up for commercial manufacturing. Because of the amorphous nature of Si-DLC and the carefully tuned plasma immersion ion implantation and deposition (PIIID) process, we achieve near complete filling of the mould (see Supplementary Information for details). This material is also expected to have significant amounts of hydrogen in addition to oxygen (31 at%) and silicon (20 at%), as measured by X-ray photoelectron spectroscopy (XPS)²⁵.

The fabricated tips were examined in a scanning electron microscope (SEM), and one such tip is shown in Fig. 1. Transmission electron microscopy (TEM) of the tips (Fig. 1d) indicated an amorphous, homogeneous material. To image the tips for comparison of wear rates, we avoided extended electron beam exposure because of suspected beam-induced carbon deposition. This is visible in the TEM image in Fig. 1c.

The wear performance of these nanoscale tips was then evaluated for sliding wear on SiO₂ in an atomic force microscope (AFM). The effects of substrate wear were minimized by carefully choosing the scan pattern (see Supplementary Information). Wear was measured *in situ* as an increase in adhesion corresponding to an increase in the contact area between the tip and substrate. This was correlated to a change in tip radius using the parameter u_{adh} (see Methods). At the macroscale, wear is a result of a combination of processes including fracture, plasticity and third-body effects, as well as atom-by-atom attrition, and has traditionally been described using Archard's phenomenological model²¹. (Archard²¹ describes the wear volume V of macroscopic plastic contacts with multiple asperities to be proportional to the load force F_N (not pressure) and sliding distance d , which can be written as $V = k_{wear} \cdot F_N \cdot d$, where k_{wear} is the dimensional wear coefficient. Bhushan later developed a similar law for elastic contacts²⁹.) However, at the nanoscale, careful studies have shown that wear can also occur in a smooth and gradual manner^{9,26}. This has been difficult to quantify until recently, when it was shown that this gradual wear process, at small size scales, is eventually limited to what is necessarily atom-by-atom attrition⁷.

Even at the nanoscale, tip wear is not necessarily limited by the strength of the atomic bonds in the material, for example, Si–Si bonds in silicon or Si–N bonds in silicon nitride, which have bond energies of up to 2.25 or 3.3 eV, respectively. Under ambient conditions, the silicon or silicon nitride surfaces terminate in a native oxide. The Si–O–Si bonds thus formed are weakened in the presence of water (hydration due to humidity such as from atmospheric humidity), and these weakened bonds are broken during the wear process^{7,27}. Sharp tips that slide on a flat surface (such as the tips in our experiments) are ideal for studying wear mechanisms in single-asperity nanoscale contacts, where the behaviour could be considerably different. A material that compares favourably with silicon under such conditions would have substantial applications, as sliding under such ambient conditions is very important for many applications of AFM tips (and for nanoelectromechanical systems (NEMS) in general). Our wear experiments using silicon tips sliding against SiO₂ result in extremely high wear rates (see Fig. 1e and Supplementary Fig. S2 for wear in silicon tips). Similar wear mechanisms due to the high silicon content in Si-DLC could adversely affect the nanoscale wear of the Si-DLC tips sliding on SiO₂. The study in ref. 28 suggests the presence of an oxygen-terminated surface on Si-DLC, which is consistent with our XPS measurements. Therefore, in spite of the well-known tribological properties of Si-DLC at the macroscale, it was not readily clear whether Si-DLC tips would indeed be superior to silicon tips at the nanoscale.

¹IBM Research - Zurich, 8803 Rüschlikon, Switzerland, ²Department of Mechanical Engineering and Applied Mechanics, University of Pennsylvania, 220 South 33rd Street, Philadelphia, Pennsylvania 19104, USA, ³Department of Engineering Physics, University of Wisconsin, 1500 Engineering Drive Madison, Wisconsin 53706, USA; †Present address: Yale University, Department of Electrical Engineering, 15 Prospect Street, New Haven, Connecticut 06511, USA (H.B.); Khon Kaen University, Industrial Engineering Department, Muang Khone Kean, Thailand 40002 (P.J.); Department of Chemistry, West Virginia University, Morgantown, West Virginia 26506, USA (Y.C.). *e-mail: bharish@umd.edu; dpt@zurich.ibm.com

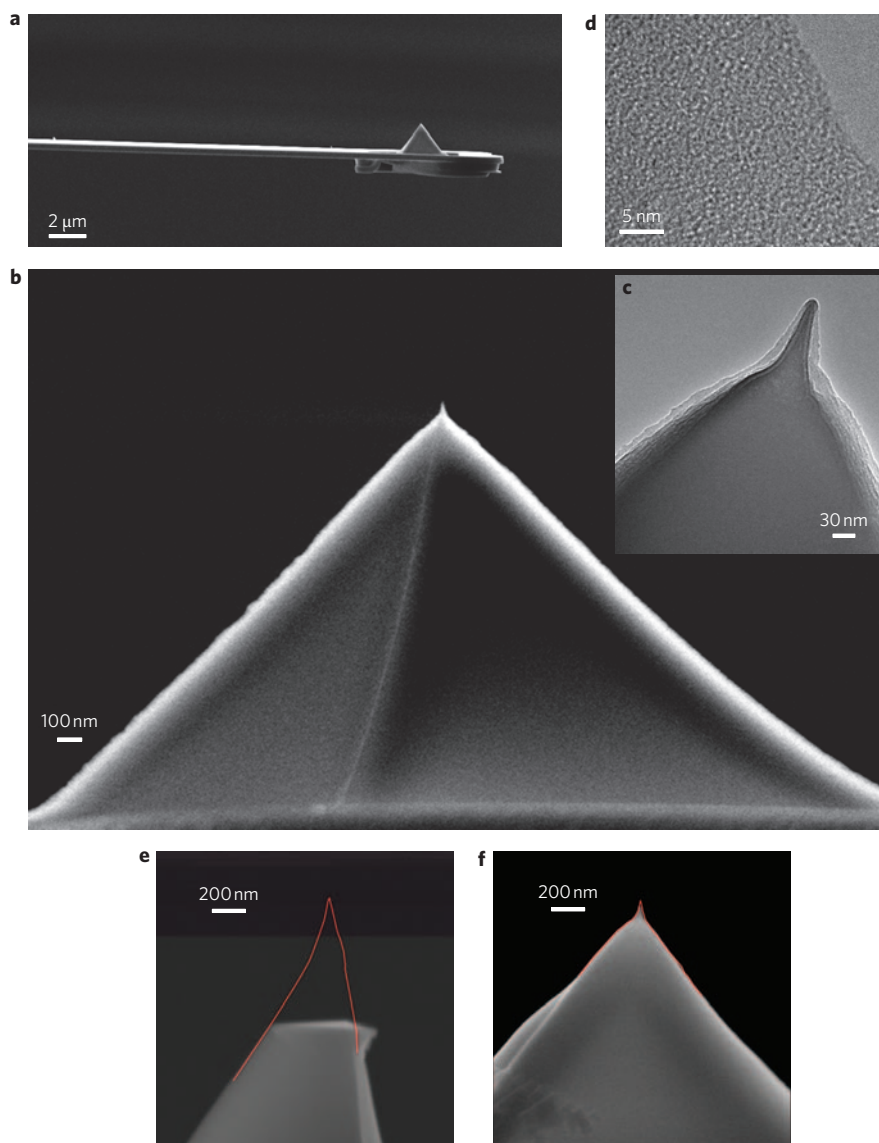


Figure 1 | Ultrasharp Si-DLC tips. **a**, SEM image of a silicon microcantilever with an ultrasharp Si-DLC tip. **b**, Close-up of the moulded tip. **c,d**, TEM images of the apex of the tip (**c**) and an edge near the apex region (**d**), showing a homogeneous amorphous structure. **e,f**, SEM images of a silicon tip (**e**) and a comparable Si-DLC tip (**f**) under similar loading and environmental conditions after 2 m of sliding wear on a SiO_2 surface. The red outline shows the tip shape before the wear experiment.

Figure 2a,c,e shows electron micrographs of three worn Si-DLC tips, with the outlines of the unworn tips (tips A, B and C) indicated by lines. From the tip images obtained in a SEM before and after wear, we estimate the wear volumes in Si-DLC to have an average value of $\sim 8.2 \times 10^3 \text{ nm}^3 \text{ m}^{-1}$ (averaged over six wear experiments), which is almost four orders of magnitude better than the wear volumes in silicon tips, which were $> 1 \times 10^8 \text{ nm}^3 \text{ m}^{-1}$ for similar sliding conditions (see Fig. 1e as well as Supplementary Fig. S5). The experimental parameters for the different wear experiments using the Si-DLC tips are summarized in Table 1.

Figure 2b,d,f shows the experimental wear data and fits for both Archard's law and the atomistic attrition model described below (as adapted from ref. 7). From the experimental data of the change of adhesion during sliding wear for the three tips in Fig. 2, it is apparent that the adhesion values change gradually, even over a large sliding distance. This indicates that there is a continual change in tip shape, consistent with the notion of an atom-by-atom wear process. However, the adhesion force is greatly influenced by there being a non-ideal surface, such as when wear debris or

contamination is present. This appears to be an issue for tip B after sliding for 0.5 m. Hence, for that particular experiment we restrict the subsequent analysis to the initial 0.5 m of sliding. The value of u_{adh} , which relates the contact area (which is proportional to the tip radius) to the pull-off force, was determined to be $2.2 (+0.2/-0.1) \text{ N m}^{-1}$ from four tips for which a high-quality image was obtained after wear, so that the contact area could be determined accurately. Assuming a slow atom-by-atom wear process, note that, from ref. 7, one can describe the atom-by-atom attrition process for a conical tip of shape $R(h)$, where h is the position along the vertical axis of the tip and d is the sliding distance, as

$$\frac{\partial R}{\partial d} = \frac{\partial R f_{\text{attempt}} b}{\partial h v} \exp\left(\frac{1}{k_B T} \{-(E_a - V_{\text{act}} \tau_0) + P \xi V_{\text{act}}\}\right) \quad (1)$$

Here, the attempt frequency, f_{attempt} , is due to phononic vibration, and the activation energy E_a is the energy required to break the bond in question, which is reduced by the sliding-induced shear

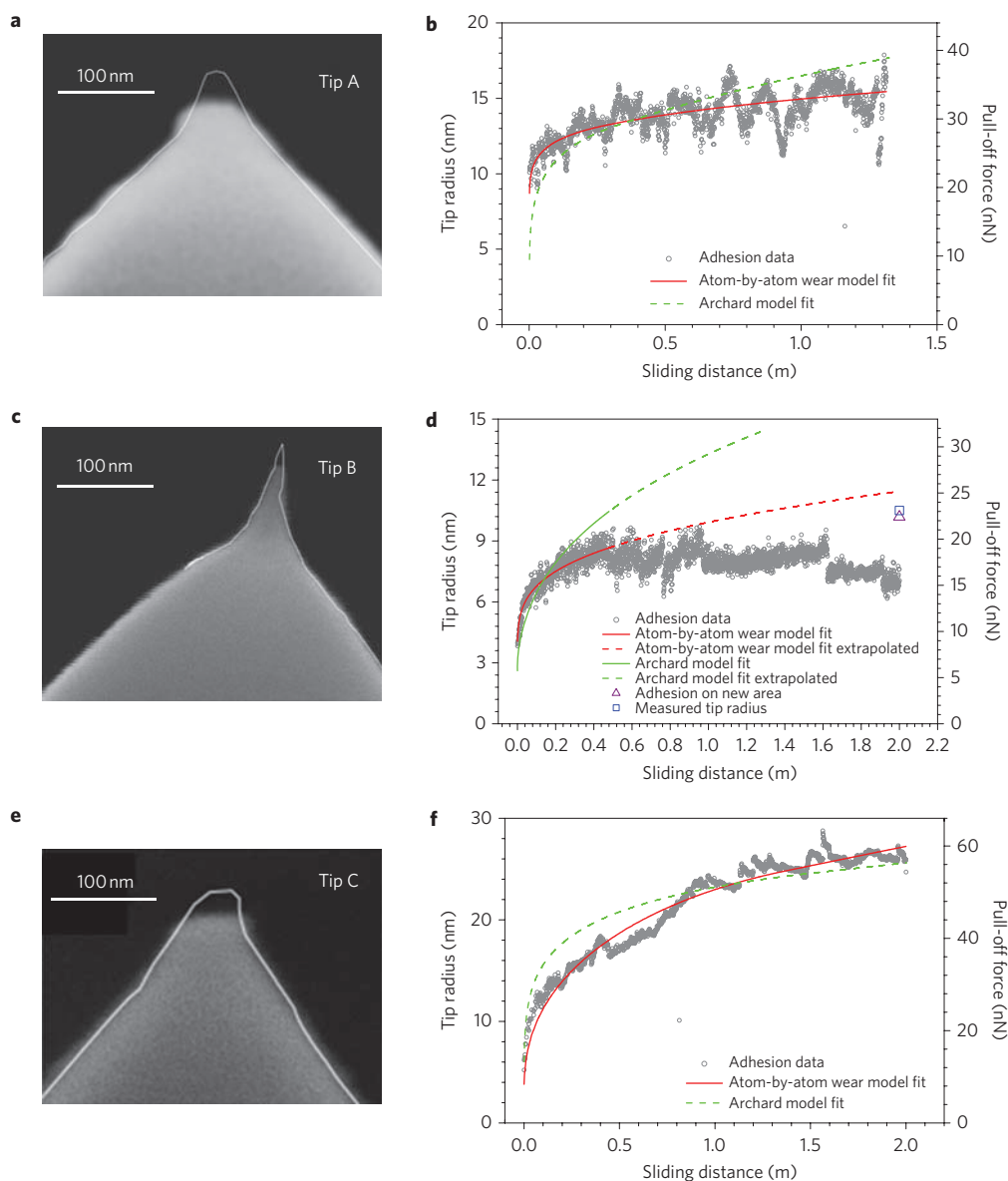


Figure 2 | Wear in Si-DLC tips sliding on SiO₂. a,c,e, SEM images of three Si-DLC tips (tips A, B and C, respectively) after the wear test, with the outline of the unworn tip indicated. b,d,f, Plots of tip radius and pull-off force (y axis) against sliding distance (x axis) for tips A, B and C. In b and f, the solid red line indicates the fit using the atomistic attrition model, and the dashed green line indicates Archard's model fit. In d, which shows the data for tip B, the adhesion force monitoring method appears to fail after 0.5 m. However, the adhesion is recovered by moving to a new area of the sample (the purple triangle), and this measured value corresponds well to the prediction of the model (fitted to 0.5 m and extrapolated). The initial fitted region is shown by the solid red line and the extrapolated region is shown by the dashed red line. The prediction of the model also matches the data for the radius (blue square). For consistency, Archard's law is fitted for the initial region (solid green line) and extrapolated for the rest of the sliding distance (dashed green line).

stress. V_{act} , k_B and T are the activation volume, Boltzmann constant and the absolute temperature, respectively. We fit this model as well as Archard's law to our experimental data. It is noted from the fits in Fig. 2 that Archard's law does not always fit our experimental data, whereas the atom-by-atom attrition model does. By fitting equation (1) to the experimental data numerically, we obtain average values of the effective activation energy, $E_{\text{net}} = E_a - V_{\text{act}}\tau_0 = 1.0 \pm 0.1$ eV, and the effective activation volume, $V_{\text{eff}} = \xi V_{\text{act}} = 3.4 (\pm 2) \times 10^{-28}$ m³ (see Methods for details of the equation fit parameters). The values of both fit parameters were very similar for all tips that were analysed (including the three tips in Supplementary Information). The sources of uncertainty for these experiments, together with the experimental parameters, are listed in Table 1. The concurrence is striking given the differences in tip shape, applied load and scan velocity. The excellent

agreement between the atomistic model fits and the experimental data provides strong support for our assumption that the wear process is indeed an atom-by-atom removal of the tip material.

By observing the rate of change of adhesion of tip B, it is seen that the adhesion is not a reliable measure of wear beyond 0.5 m of sliding in this experiment. We suspect that this was due to wear debris (caused by the wear) or contamination (caused by either undesirable adsorbents or other ambient contaminants) on the surface, which changes either the work of adhesion or the contact geometry (or both). Hence, we fit this data only up to 0.5 m. We then extrapolated this fit to 2 m. The model predicts a tip radius of 12 nm for this sliding distance, corresponding to a pull-off force of 25.5 nN. Our post-wear measurement of the tip radius in a SEM was 11 nm. After the experiment, the force of adhesion was also measured in a new area of the sample surface to rule out

Table 1 | Summary of experimental and model fit parameters for Si-DLC tips.

DLC tip	Starting radius* (nm)	End radius† (nm)	Sliding velocity ($\mu\text{m s}^{-1}$)	Applied load (nN)	Wear volume ($\text{nm}^3 \text{m}^{-1}$)	E_{net} (eV)	V_{eff} (10^{-28}m^3)	Sources of error‡
A	11.2	18.3	250	17.5	8.5×10^3	1.0 ± 0.05	2.4 ± 0.06	c
B	4	11	10	1.35	1.6×10^3	1.0 ± 0.07	1.6 ± 0.06	a, b, c
C	26.4	25^{\S}	10	1.15	11.8×10^3	0.97 ± 0.03	$0.4 + 0.6/-0.2$	a, c

*Radius of the spherical termination of the unworn tip.

†Radius of the flat end of the worn tip.

‡a = u_{adh} ; b = contamination; c = k (cantilever stiffness).

§The starting radius is larger, because in this case, after wear, the tip had not yet worn down past the half-sphere.

effects of wear debris. By measuring this force at ten independent points, away from the area in which the tip was previously worn, we obtained a pull-off force of 23 ± 1.5 nN. Both parameters agree well with the model prediction, thus supporting both the validity of the model and our hypothesis that the wear debris or contamination plays a role. This is further evidence that this model can be used to predict accurately the lifetime of nanoscale components in sliding wear. Thus, although the adhesion method of measuring wear *in situ* sometimes becomes unreliable after an initial sliding period, this method can still be a reliable measure of wear in such situations, if only the initial part of the data is used. (This is also seen in tip E in the Supplementary Information.)

In Fig. 3, we plot the variation of the wear rate as the tip wears for tip A. Some previous reports observed that the wear rates of AFM tips change as a function of time^{8,9,26}. For these tip wear experiments, it was found that the wear rate changes as a function of tip size (or pressure under the tip). For tip A, the wear rate changes from $\sim 2 \times 10^{-6} \text{mm}^3 \text{N}^{-1} \text{m}^{-1}$ at the beginning of the experiments and decreases to almost $1 \times 10^{-8} \text{mm}^3 \text{N}^{-1} \text{m}^{-1}$ after sliding for 2 m. Archard's law predicts identical wear rates for identical loads, even if the contact geometries (and thus the applied pressures) are different. Although constant wear rates are not always observed in macroscopic sliding contacts, the gradual change of rate of momentary wear that we observe is distinctly different from the transient run-in effects often observed in macroscopic systems. Therefore, to compare the wear volumes, (that is, implicitly applying Archard's wear law) can be misleading. In the case of tips for which the geometry is well defined (that is, conical AFM tips as in our experiment), the atom-by-atom attrition model can be used to make predictions about sliding distances that would result in a certain diameter at the tip apex. Note that, in Fig. 3, the wear rates of the blunted tip A agree very well with a macroscopic wear rate for the same Si-DLC film sliding on a

similar tribochemical system (Si_3N_4) of $1 \times 10^{-8} \text{mm}^3 \text{N}^{-1} \text{m}^{-1}$ (ref. 27). Our experiments provide evidence that the wear rate differs significantly at very small length scales, but may converge to the macroscopic wear rate for very blunt tips.

To make a meaningful comparison of the wear resistance of Si-DLC and silicon tips, we used the model to predict that the Si-DLC tips would, on average, slide 3.18 km (compared to 2 m) before they exhibit a diameter comparable to that of a silicon tip (silicon tip A) sliding for 2 m. Thus, the model predicts one order of magnitude lower wear resistance compared to the wear volume comparison ($\sim 1 \times 10^4$), as the wear volume computation assumes constant wear rates, which is not the case for nanoscale contacts. In both cases, however, the improvement of Si-DLC over silicon is dramatic and can be attributed to several mechanisms. The C–C and C=C bonds (3.6 and 6.4 eV bond enthalpies, respectively) are among the strongest of any atomic pair, and together with Si–C (3.3 eV) and Si–O (5.82 eV) are much stronger than the Si–Si bond (2.38 eV). Furthermore, the low friction of Si-DLC reduces the shear stress τ , thus increasing the effective activation barrier for atom-by-atom attrition. Also, the use of Si-DLC changes the surface chemistry when compared to that of the silicon tip, potentially eliminating tribochemical etching of the tip in ambient humidity. Our experiments were carried out in ambient humidity, and the extremely high wear rates of SiO_2 in such conditions are well documented²⁹. The experimental data for Si-DLC show little wear and suggest that if this layer consists of SiO_2 , it does not reform on the Si-DLC surface. From Fig. 3, one can estimate the number of atoms lost per scan frame of a typical AFM image (~ 1 mm sliding at an applied force of 1 nN) to be on the order of 1,000 atoms, that is, equal to one atom for every micrometre of sliding.

In summary, we have achieved very low wear rates in Si-DLC at the nanoscale. We have quantified this wear using an atom-by-atom attrition model and estimate the activation energies in sliding wear against SiO_2 to be 1.0 ± 0.1 eV, with an average activation volume of $3.4 \times 10^{-28} \pm 2 \times 10^{-28} \text{m}^3$. Future studies would test the limits of the applicability of the atom-by-atom wear model. For instance, if the shear stress component τ were known (using friction experiments), one could estimate the activation volume, V_{act} . The activation volume can be thought of as a kinetic signature of the wear mechanism¹². This would in turn provide all the elements required to completely describe the process of material attrition at the nanoscale. Nanoscale components with single-asperity contacts have posed a number of novel tribological challenges, and mitigating some of these issues goes hand in hand with better descriptions of the physical mechanisms that govern this process.

Methods

Fabrication of cantilevers with ultrasharp, monolithic Si-DLC tips. We fabricated silicon cantilevers with Si-DLC tips using a moulding technique on a {100} silicon-on-insulator wafer (SOI). The moulds were formed within the handle (or bottom substrate) of the wafer (Supplementary Fig. S2) by etching along the {111} planes (self-limiting in KOH). Subsequently, the moulds were sharpened by thermal oxidation. This was followed by the Si-DLC deposition step, in which the Si-DLC was deposited in a hexamethyl disiloxane (HMDSO) precursor gas using a plasma

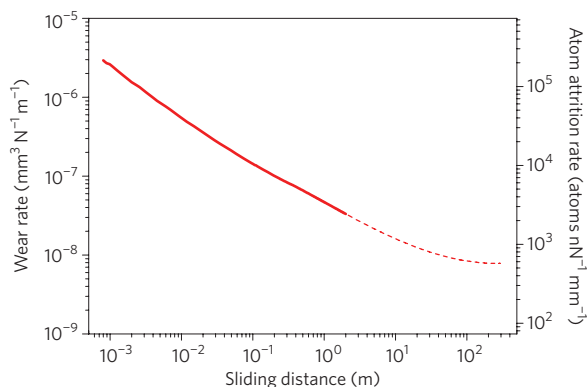


Figure 3 | Rate of wear as a function of sliding distance for tip A. The solid line to the left is from the fits to the experimental data, and the dotted line to the right is the extrapolation of the data using the atom-by-atom attrition model. The wear rate changes over three orders of magnitude over the course of the experiment.

immersion ion implantation and deposition (PIIID) process^{30–32}. The plasma was created by a glow discharge method, and a relatively low-energy (–5 kV) deposition was used to deposit the Si-DLC. The non-line-of-sight nature of the PIIID process allows uniform ion implantation or film deposition on three-dimensional parts, such as the sharpened mould. The Si-DLC was then etched in SF₆ plasma to restrict the Si-DLC to a region immediately around the tip (see etch process details in the Supplementary Information). The cantilever was defined on the device layer of the SOI wafer, followed by a back-side, deep reactive ion etch of the handle. Subsequently, it was released in buffered hydrofluoric acid, which was also expected to remove any silicon oxides from the sharpening step.

Determination of the cantilever spring constant k . The normal force spring constants (k) of the cantilevers are necessary to determine the force applied for a given deflection. Much more importantly, they are also necessary to determine the adhesion. The determination of k is a source of uncertainty in measurements and depends on the particular cantilever used. To minimize the uncertainty, we used several methods to determine k . The cantilever frequency and Q were determined by frequency tuning of the cantilever in a commercial AFM. This information can be used to calculate k using Sader's method³³. However, this method sometimes produces unrealistic k values, in which case the spring constant that is calculated from a simple geometrical measurement of the cantilever (length to tip, width and thickness) is used. If reliable geometry data are not available, we use the value of the final force of adhesion and the known value of u_{adh} as established through other more reliable measurements to determine the pull-off force.

Wear experiment. Using a custom-built AFM, we investigated the wear of Si-DLC tips at different velocities and loading conditions (listed in Table 1). The SiO₂ sample used in this experiment was thermally grown on a prime-grade silicon wafer in an oxidation furnace, and had a thickness of 500 nm. The resulting oxide surface had a roughness of <0.2 nm (r.m.s.). Experiments were carried out in ambient conditions, and measured temperatures were 295 ± 5 K with a relative humidity $30 + 11/ - 5\%$. We tried to avoid the effects of substrate wear by scanning different lines (see Supplementary Information, 'Tip Wear Scan Protocol', for details). Measuring the tip shape during the wear experiment is important to gain more insight into the wear process. For this, electron microscopy is too slow. Instead, the adhesion between tip and surface, as measured in a simple pull-off (or force–distance) experiment, can be used as an indicator of *in situ* wear. To a first approximation, the adhesion force between a flattened tip and a flat surface is proportional to the contact radius R (which is the tip radius for a flat tip, as would be the case in worn tips) with a constant u_{adh} , and can be written as $F_{\text{adh}} = u_{\text{adh}}R$ (ref. 7). We configured the AFM to collect adhesion data in an automatic manner after every 0.8 mm of sliding, while keeping the force at the tip almost constant (variations of less than 1% from the desired force).

Model fitting. In the context of fitting the atomistic attrition model, the shear stress τ is a function of applied pressure P and depends on temperature T and velocity v . It can be written as $\tau = \tau_0 + \xi P + k_B T / V_{\text{act}} \ln(v/v_0)$, where τ_0 , ξ and v_0 are constants. The average pressure P is given by total force at the tip (the sum of applied and adhesive load), divided by the contact area, πR^2 . The velocity dependence of the shear stress (third term) has been shown to be of minor consequence in friction and wear for the velocities involved in the experiments described here^{10,34}, so we ignored the velocity dependence of the shear stress (not the wear rate) for this analysis. We therefore fit our experiments using a pressure-dependent shear stress $\tau = \tau_0 + \xi P$. Equation (1) can be numerically fit to the experimental data by varying two parameters: the effective activation energy, $E_{\text{net}} = E_a - V_{\text{act}}\tau_0$, and an effective activation volume, $V_{\text{eff}} = \xi V_{\text{act}}$. The unworn tip geometry $R(h)$ is approximated by a cone truncated in a sphere, the radius of which was measured using SEM images. Note that V_{eff} is the activation volume altered by the pressure dependence constant ξ .

Received 22 October 2009; accepted 8 January 2010;
published online 31 January 2010

References

- Persson, B. N. J. *Sliding Friction* (Springer, 2000).
- Gnecco, E. *Fundamentals of Friction and Wear on the Nanoscale* (Springer, 2006).
- Mo, Y., Turner, K. T. & Szuflarska, I. Friction laws at the nanoscale. *Nature* **457**, 1116–1119 (2009).
- Gnecco, E. *et al.* Velocity dependence of atomic friction. *Phys. Rev. Lett.* **84**, 1172–1175 (2000).
- Bhushan, B., Israelachvili, J. N. & Landman, U. Nanotribology: friction, wear and lubrication at the atomic scale. *Nature* **374**, 607–616 (1995).
- Carpick, R. W. & Salmeron, M. Scratching the surface: fundamental investigations of tribology with atomic force microscopy. *Chem. Rev.* **97**, 1163–1194 (1997).
- Gotsmann, B. & Lantz, M. A. Atomistic wear in a single asperity sliding contact. *Phys. Rev. Lett.* **101**, 125501 (2008).
- Bennewitz, R. & Dickinson, J. T. Fundamental studies of nanometer-scale wear mechanisms. *MRS Bull.* **33**, 1174–1180 (2008).
- Maw, W., Stevens, F., Langford, S. C. & Dickinson, J. T. Single asperity tribochemical wear of silicon nitride studied by atomic force microscopy. *J. Appl. Phys.* **92**, 5103–5109 (2002).
- Bhushan, B. & Kwak, K. J. Velocity dependence of nanoscale wear in atomic force microscopy. *Appl. Phys. Lett.* **91**, 163113 (2007).
- Gnecco, E., Bennewitz, R. & Meyer, E. Abrasive wear on the atomic scale. *Phys. Rev. Lett.* **88**, 215501 (2002).
- Zhu, T., Li, J., Ogata, S. & Yip, S. Mechanics of ultra-strength materials. *MRS Bull.* **34**, 167–172 (2009).
- Luan, B. & Robbins, M. O. The breakdown of continuum models for mechanical contacts. *Nature* **435**, 929–932 (2005).
- Grill, A. Review of the tribology of diamond-like carbon. *Wear* **168**, 143–153 (1993).
- Erdemir, A. & Donnet, C. Tribology of diamond-like carbon films: recent progress and future prospects. *J. Phys. D* **39**, R311–R327 (2006).
- Neuville, S. & Matthews, A. A perspective on the optimisation of hard carbon and related coatings for engineering applications. *Thin Solid Films* **515**, 6619–6653 (2007).
- Robertson, J. Diamond-like amorphous carbon. *Mater. Sci. Eng. R* **37**, 129–281 (2002).
- Bowden, F. P. & Hanwell, A. E. Friction and wear of diamond in high vacuum. *Nature* **201**, 1279–1281 (1964).
- Donnet, C. & Erdemir, A. *Tribology of Diamond-Like Carbon Films* (Springer, 2007).
- Bhushan, B. *Modern Tribology Handbook* (CRC Press, 2001).
- Archard, J. F. Contact and rubbing of flat surfaces. *J. Appl. Phys.* **24**, 981–988 (1953).
- Niedermann, P. *et al.* CVD diamond probes for nanotechnology. *Appl. Phys. A* **66**, S31–S34 (1998).
- Oesterschulze, E. *et al.* Fabrication of small diamond tips for scanning probe microscopy application. *Appl. Phys. Lett.* **70**, 435–437 (1997).
- Kim, K. *et al.* Novel ultrananocrystalline diamond probes for high-resolution low-wear nanolithographic techniques. *Small* **1**, 866–874 (2005).
- Grierson, D. S. Nanotribological properties of nanostructured hard carbon thin films. PhD thesis, Univ. Wisconsin (2008).
- Chung, K. & Kim, D. Fundamental investigation of micro wear rate using an atomic force microscope. *Tribol. Lett.* **15**, 135–144 (2003).
- Bares, J., Sumant, A., Grierson, D., Carpick, R. & Sridharan, K. Small amplitude reciprocating wear performance of diamond-like carbon films: dependence of film composition and counterface material. *Tribol. Lett.* **27**, 79–88 (2007).
- Choi, J., Kawaguchi, M., Kato, T. & Ikeyama, M. Deposition of Si-DLC film and its microstructural, tribological and corrosion properties. *Microsyst. Technol.* **13**, 1353–1358 (2007).
- Bhushan, B. *Introduction to Tribology* (Wiley, 2002).
- Anders, A. *Handbook of Plasma Immersion Ion Implantation and Deposition* (Wiley-Interscience, 2000).
- Reeber, R. R. O. & Sridharan, K. O. W. Plasma source ion implantation. *Adv. Mater. Proc.* **146**, 21–23 (1994).
- Glocker, D. A. & Shah, S. I. *Handbook of Thin Film Process Technology* (Institute of Physics Publishing, 1995).
- Sader, J. E., Chon, J. W. M. & Mulvaney, P. Calibration of rectangular atomic force microscope cantilevers. *Rev. Sci. Instrum.* **70**, 3967–3969 (1999).
- Tambe, N. S. & Bhushan, B. Friction model for the velocity dependence of nanoscale friction. *Nanotechnology* **16**, 2309–2324 (2005).

Acknowledgements

H.B. and A.S. acknowledge the experimental support of W. Haeberle, M. Pedo and P. Baechtold. The authors thank C. Bolliger for proofreading the manuscript. H.B. acknowledges partial support from the European Commission through grant no. FP6-2005-IST-5-34719 for the project ProTeM. R.W.C. acknowledges partial support provided for this research by the Nano/Bio Interface Center through the National Science Foundation NSEC DMR-0425780.

Author contributions

H.B. wrote this manuscript with inputs from all authors. H.B. and B.G. analysed the data, with participation of M.A.L. H.B., U.D. and M.D. participated in the fabrication of the cantilevers. Y.C. and K.S. optimized the plasma process parameters for deposition and performed the deposition. P.J. performed the TEM imaging of the tips and with R.W.C. interpreted the results of TEM. H.B., B.G., A.S., R.W.C. and M.A.L. designed the wear experiment. H.B. and A.S. performed the experiments and collected the data. H.B., B.G., M.A.L. and R.W.C. analysed and interpreted the results.

Additional information

The authors declare no competing financial interests. Supplementary information accompanies this paper at www.nature.com/naturenanotechnology. Reprints and permission information is available online at <http://npg.nature.com/reprintsandpermissions/>. Correspondence and requests for materials should be addressed to H.B. and M.D.